A NUMERICAL MODEL FOR UNILATERAL MATERIALS IN FINITE DEFORMATIONS, PART II: FINITE ELEMENT IMPLEMENTATION AND APPLICATIONS

Massimo Cuomo
Mario Fagone

ABSTRACT

The implementation of the model for unilateral no-Tension materials described in part one in a standard isoparametric nonlinear finite elements code is described and discussed. A formulation based on the tensorial components of the Cauchy-Green deformation tensor has been used. Explicit expressions for the components of the material and geometric tangent stiffness matrices and for the equivalent internal nodal forces are furnished. Special attention has been focused on the material tangent stiffness matrix, in order to obtain satisfactory convergence properties. Some examples complete the paper.

INTRODUCTION

In this paper the finite element implementation of the No Tension Material (NTM) model proposed in [1] is described. The numerical model can be used to describe the behaviour of materials like masonry, unreinforced concrete, mortar, sand, soft rock, that have very low tensile resistance, generally neglected in engineering applications. The classical multiplicative decomposition of the deformation gradient has been used to schematise the deformation process. The constitutive relations have been developed according to the maximum dissipation principle. On this way a continuous tensor field is defined accounting for anelastic effects [2].

The set of constitutive relations and the compatibility condition have been enforced using a Newton-Raphson integration scheme. Particular attention have been paid to determine of the right expression of the algorithm tangent moduli to ensure quadratic rate of convergence to the global FE model.

Either a Total Lagrangian (TL) and an Updated Lagrangian (UL) implementations of the model are discussed in the paper [3,4]. The TL formulation is based on stress and velocity measures defined in the reference fixed configuration, while the UL formulation is based on the same objects defined in the current configuration. For both

formulations explicit expressions for the equivalent nodal forces and for the geometric and material stiffness matrices are reported.

The UL formulation has been implemented in a FE code and some applications have shown the usefulness of the model comparing the results with those given by standard codes. Some of the results appear to confirm the original motivation of the paper, i.e. the necessity of performing a full large deformation analysis for No-Tension structures in order to properly account for its nonlinear response.

THE MATERIAL MODEL

Kinematics

In this paper the No Tension Materials model described in [1] is considered. Here only the basic relations that define the model are reported.

In order to account for anelastic effects the classical multiplicative decomposition of the deformation gradient is used, so that the deformation process is split in its elastic and anelastic parts introducing an intermediate stress free configuration B_a between the initial (B_0) and final (B_t) configurations (see Figure 1 of [1]).

Consequently the gradient of deformation is multiplicatively split in

$$\mathbf{F} = \mathbf{F}_e \mathbf{F}_a \qquad J = J_e J_a \tag{1}$$

Different measures of deformation and velocity of deformation are defined in each configuration. The more relevant deformation tensors are reported in the following relations

$$\mathbf{C} = \mathbf{F}_a^T \mathbf{F}_e^T \mathbf{F}_e \mathbf{F}_a = \mathbf{F}_a^T \mathbf{C}_e \mathbf{F}_a \tag{2}$$

$$\mathbf{C}_a = \mathbf{F}_a^T \mathbf{F}_a \tag{3}$$

$$\mathbf{l} = \nabla_{\underline{x}} \underline{v} = \dot{\mathbf{F}} \mathbf{F}^{-1} = \dot{\mathbf{F}}_e \mathbf{F}_e^{-1} + \mathbf{F}_e \dot{\mathbf{F}}_a \mathbf{F}_a^{-1} \mathbf{F}_e^{-1} = \mathbf{l}_e + \mathbf{l}_a = \mathbf{F}_e \hat{\mathbf{l}}_e \mathbf{F}_e^{-1} + \mathbf{F}_e \hat{\mathbf{l}}_a \mathbf{F}_e^{-1} \tag{4}$$

$$\hat{\mathbf{l}} = \mathbf{F}_e^{-1} \mathbf{l} \mathbf{F}_e = \mathbf{F}_e^{-1} \dot{\mathbf{F}} \mathbf{F}^{-1} \mathbf{F}_e = \mathbf{F}_e^{-1} \dot{\mathbf{F}}_e + \dot{\mathbf{F}}_a \mathbf{F}_a^{-1} = \hat{\mathbf{l}}_e + \hat{\mathbf{l}}_a \tag{5}$$

$$\mathbf{d} = \mathrm{sym}(\mathbf{l}) \qquad \hat{\mathbf{d}} = \mathrm{sym}(\mathbf{C}_e \hat{\mathbf{l}}) = \mathbf{F}_e^T \mathbf{d} \mathbf{F}_e \tag{6}$$

In (6), $\hat{\mathbf{d}}$ is the symmetric part of the covariant form of the velocity of deformation defined in B_a, obtained pre-multiplying $\hat{\mathbf{l}}$ (a mixed variant tensor) by the convective metric $\mathbf{C}_e$ (that is different from the metric relative to the reference frame defined in the intermediate configuration) [5]. Note that $\hat{\mathbf{l}}_a = \dot{\mathbf{F}}_a \mathbf{F}_a^{-1}$ gives the evolution of the intermediate configuration V_a.

It is well known that we can use different stress measures referred to the different configurations to describe the stress state

$$\sigma \quad \text{Cauchy stres tensor} \tag{7}$$

$$\tau = J\sigma \quad \text{Kirchhoff stress tensor} \tag{8}$$

$$\mathbf{P} = \tau \mathbf{F}^{-T} \text{ I Piola Kirchhoff - nominal stress tensor} \tag{9}$$

$$\mathbf{S} = \mathbf{F}^{-1} \tau \mathbf{F}^{-T} \text{ II Piola Kirchhoff stress tensor} \tag{10}$$

14

$$\mathbf{S}_e = \mathbf{F}_e^{-1} \tau \mathbf{F}_e^{-T} \text{ "elastic" stress tensor} \tag{11}$$

As objective stress rates the material derivative of the second Piola Kirchhoff stress tensor (defined in the reference fixed configuration), and the Lie derivative of the stress tensors defined in the intermediate and in the final configuration are used

$$L_v^p \mathbf{S}_e = \left\{ \mathbf{F}_a \frac{\partial}{\partial t} \Big[\mathbf{F}_a^{-1} (\mathbf{S}_e \circ \varphi_a) \mathbf{F}_a^{-T} \Big] \mathbf{F}_a^T \right\} \circ \varphi_a^{-1} = \dot{\mathbf{S}}_e - \hat{\mathbf{l}}_a \mathbf{S}_e - \mathbf{S}_e \hat{\mathbf{l}}_a^T \tag{12}$$

$$L_v \tau = \left\{ \mathbf{F} \frac{\partial}{\partial t} \Big[\mathbf{F}^{-1} (\tau \circ \varphi) \mathbf{F}^{-T} \Big] \mathbf{F}^T \right\} \circ \varphi^{-1} = \dot{\tau} - \mathbf{l}\tau - \tau \mathbf{l}^T = \mathbf{F}_e L_v^p \mathbf{S}_e \mathbf{F}_e^T \tag{13}$$

Constitutive Model

The constitutive model for No Tension Materials is obtained considering that in the material tension stresses are not allowed and assuming that no dissipation occurs in the anelastic process, so that it is defined by the following conditions:

1. the stress state is admissible if the maximum (true) Cauchy stress is not positive

$$\sigma_{n\,max} \leq 0 \tag{14}$$

Since $J \geq 0$ always (14) is equivalent to

$$\tau_{n\,max} \leq 0 \tag{15}$$

2. null anelastic dissipations

$$D = \tau \cdot \mathbf{l}_a = \tau \cdot \mathbf{d}_a = 0 \tag{16}$$

the previous formula implies that the anelastic deformations grows in the direction of the maximum eigenvalue of the stress tensor $\boldsymbol{\sigma}$ (that has the same principal direction as $\boldsymbol{\tau}$). Differently from the small deformation model, since the admissibility condition (15) is referred to the deformed configuration, the constitutive law is expressed in the current configuration in incremental form, as

$$\begin{array}{cc} \mathbf{l}_a = \mathbf{d}_a = \dot{\beta} \partial_\tau f(\tau) & f(\tau) = \tau_{n\,max} \\ g(\tau) \leq 0 & \dot{\beta} f(\tau) = 0 \end{array} \tag{17}$$

Note that the condition $\mathbf{l}_a = \dot{\beta} \partial_\tau f(\tau) = \mathbf{d}_a$ follows from request (16) and implies that the spin tensor must be zero. Using the identity $D = \tau \cdot \mathbf{d}_a = \mathbf{S}_e \cdot \hat{\mathbf{d}}_a$ and Equation (11), the constitutive relations (17) can be formulated in the intermediate configuration as:

$$\hat{\mathbf{l}}_a = \mathbf{C}_e \hat{\mathbf{l}}_a = \dot{\beta} \frac{\partial \hat{f}(\mathbf{S}_e)}{\partial \mathbf{S}_e} = \hat{\mathbf{d}}_a \tag{18}$$

since $\qquad sym(\mathbf{d}_a) = \dot{\beta} \dfrac{\partial \hat{f}(\tau(\mathbf{S}_e))}{\partial \tau} = \dot{\beta} \mathbf{F}_e^{-T} \dfrac{\partial \hat{f}(\mathbf{S}_e)}{\partial \mathbf{S}_e} \mathbf{F}_e^{-1} = \mathbf{F}_e^{-T} \hat{\mathbf{d}}_a \mathbf{F}_e^{-1}$ (19)

FINITE ELEMENT IMPLEMENTATION

Interpolation Operators

The model is implemented using a FE isoparametric formulation. Cartesian frameworks only are used and we restrict ourselves to 2D problems. The shape functions (g_i) are defined in an parent element domain V_ξ (see Figure 1, [4]), so that the following interpolating relations are used for the position vectors $\underline{\mathbf{X}}$ and $\underline{\mathbf{x}}$ in the reference and current configuration respectively:
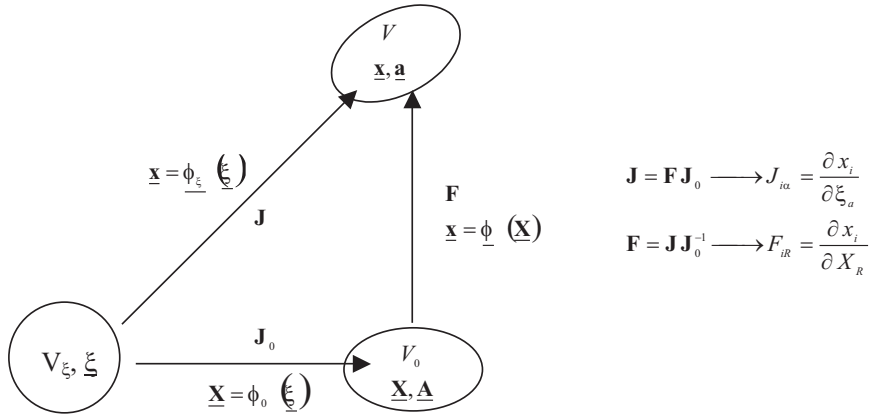
Figure 1. Configuration Mapping

$$\mathbf{N}(\underline{\xi}):=\begin{bmatrix} g_1(\underline{\xi})\cdots g_n(\underline{\xi}) & 0 \\ 0 & g_1(\underline{\xi})\cdots g_n(\underline{\xi}) \end{bmatrix} \tag{20}$$

$$\underline{\mathbf{x}}(\underline{\xi},t)=\begin{bmatrix} x_1(\underline{\xi},t) \\ x_2(\underline{\xi},t) \end{bmatrix}=\mathbf{N}(\underline{\xi})\begin{bmatrix} \underline{\mathbf{a}}_1(t) \\ \underline{\mathbf{a}}_2(t) \end{bmatrix} \qquad \underline{\mathbf{X}}(\underline{\xi})=\begin{bmatrix} X_1 \\ X_2 \end{bmatrix}=\mathbf{N}(\underline{\xi})\begin{bmatrix} \underline{\mathbf{A}}_1 \\ \underline{\mathbf{A}}_2 \end{bmatrix} \tag{21}$$

In the above, g_i is the i-th shape function and $\underline{\mathbf{A}}_i$ and $\underline{\mathbf{a}}_i$ are the reference and current nodal position vectors in the i-th direction. The indices 1, 2 refer to the component of the nodal variable in the Cartesian reference system.

The Jacobian $\mathbf{J}_0=\nabla_\xi\mathbf{X}$ is evaluated as follows:

$$\mathbf{J}_0=\begin{bmatrix} \left(\overline{\mathbf{B}}_\xi^T\underline{\mathbf{A}}_1\right)^T \\ \left(\overline{\mathbf{B}}_\xi^T\underline{\mathbf{A}}_2\right)^T \end{bmatrix}=\begin{bmatrix} \underline{\mathbf{A}}_1^T\overline{\mathbf{B}}_\xi \\ \underline{\mathbf{A}}_2^T\overline{\mathbf{B}}_\xi \end{bmatrix} \quad \text{with} \quad \overline{\mathbf{B}}_\xi=\begin{bmatrix} \dfrac{\partial g_1}{\partial\xi_1} & \dfrac{\partial g_1}{\partial\xi_2} \\ \vdots & \vdots \\ \dfrac{\partial g_n}{\partial\xi_1} & \dfrac{\partial g_n}{\partial\xi_2} \end{bmatrix} \tag{22}$$

The gradient of deformation and gradient of velocity tensors are then interpolated as:

$$\mathbf{F} = \begin{bmatrix} \left(\overline{\mathbf{B}}^T \underline{\mathbf{a}}_1\right)^T \\ \left(\overline{\mathbf{B}}^T \underline{\mathbf{a}}_2\right)^T \end{bmatrix} = \begin{bmatrix} \underline{\mathbf{a}}_1^T \overline{\mathbf{B}} \\ \underline{\mathbf{a}}_2^T \overline{\mathbf{B}} \end{bmatrix} \text{ with } \overline{\mathbf{B}} = \begin{bmatrix} \dfrac{\partial g_1}{\partial X_1} & \dfrac{\partial g_1}{\partial X_2} \\ \vdots & \vdots \\ \dfrac{\partial g_n}{\partial X_1} & \dfrac{\partial g_n}{\partial X_2} \end{bmatrix} \longrightarrow \begin{aligned} \overline{B}_{iR} &= \dfrac{\partial g_i}{\partial \xi_\alpha} \dfrac{\partial \xi_\alpha}{\partial X_R} = \dfrac{\partial g_i}{\partial \xi_\alpha} J_{0\ \alpha R}^{-1} \\[2mm] \overline{\mathbf{B}} &= \overline{\mathbf{B}}_\xi \, \mathbf{J}_0^{-1} \end{aligned} \quad (23)$$

$$\mathbf{l} = \nabla_{\underline{x}}(\mathbf{v}) = \nabla_{\underline{X}}(\mathbf{v}) \nabla_{\underline{x}} \underline{\mathbf{X}} = \nabla_{\underline{x}}\left(\mathbf{N}(\xi)\right) \underline{\dot{\mathbf{a}}} \, \mathbf{F}^{-1} = \begin{bmatrix} \left(\mathbf{F}^{-T} \overline{\mathbf{B}}^T \underline{\dot{\mathbf{a}}}_1\right)^T \\ \left(\mathbf{F}^{-T} \overline{\mathbf{B}}^T \underline{\dot{\mathbf{a}}}_2\right)^T \end{bmatrix} \quad (24)$$

In the follow we will reckon the equivalent nodal forces and the stiffness matrix using the virtual power equation, in which scalar product of tensors are present. Computationally it is useful to perform this operations in vector form using Voigt notation. In this notation the components of the material deformation and of the velocity of deformation tensors (see Equation (24)) are interpolated as

$$\mathbf{E} = \frac{1}{2}\left(\mathbf{F}^T \mathbf{F} - \mathbf{I}\right) \rightarrow \underline{\dot{\mathbf{E}}} = \begin{pmatrix} \dot{E}_{11} \\ \dot{E}_{22} \\ 2\dot{E}_{12} \end{pmatrix} = \mathbf{B}_0^T \underline{\dot{\mathbf{a}}} \qquad \mathbf{d} = sym(\mathbf{l}) \rightarrow \underline{\mathbf{d}} = \begin{pmatrix} d_{11} \\ d_{22} \\ 2d_{12} \end{pmatrix} = \mathbf{B}_\Omega^T \underline{\dot{\mathbf{a}}} \quad (25)$$

where

$$\mathbf{B}_0 = \begin{bmatrix} \overline{B}_{11}\overline{B}_{j1}a_j^{(1)} & \overline{B}_{12}\overline{B}_{j2}a_j^{(1)} & \overline{B}_{11}\overline{B}_{j2}a_j^{(1)} + \overline{B}_{12}\overline{B}_{j1}a_j^{(1)} \\ \vdots & \vdots & \vdots \\ \overline{B}_{n1}\overline{B}_{j1}a_j^{(1)} & \overline{B}_{n2}\overline{B}_{j2}a_j^{(1)} & \overline{B}_{n1}\overline{B}_{j2}a_j^{(1)} + \overline{B}_{n2}\overline{B}_{j1}a_j^{(1)} \\ \overline{B}_{11}\overline{B}_{j1}a_j^{(2)} & \overline{B}_{12}\overline{B}_{j2}a_j^{(2)} & \overline{B}_{11}\overline{B}_{j2}a_j^{(2)} + \overline{B}_{12}\overline{B}_{j1}a_j^{(2)} \\ \vdots & \vdots & \vdots \\ \overline{B}_{n1}\overline{B}_{j1}a_j^{(2)} & \overline{B}_{n2}\overline{B}_{j2}a_j^{(2)} & \overline{B}_{n1}\overline{B}_{j2}a_j^{(2)} + \overline{B}_{n2}\overline{B}_{j1}a_j^{(2)} \end{bmatrix} \quad \mathbf{B}_\Omega = \begin{bmatrix} \left(\overline{\mathbf{B}}\mathbf{F}^{-1}\right)_{11} & 0 & \left(\overline{\mathbf{B}}\mathbf{F}^{-1}\right)_{12} \\ \vdots & \vdots & \vdots \\ \left(\overline{\mathbf{B}}\mathbf{F}^{-1}\right)_{n1} & 0 & \left(\overline{\mathbf{B}}\mathbf{F}^{-1}\right)_{n2} \\ 0 & \left(\overline{\mathbf{B}}\mathbf{F}^{-1}\right)_{12} & \left(\overline{\mathbf{B}}\mathbf{F}^{-1}\right)_{11} \\ \vdots & \vdots & \vdots \\ 0 & \left(\overline{\mathbf{B}}\mathbf{F}^{-1}\right)_{n2} & \left(\overline{\mathbf{B}}\mathbf{F}^{-1}\right)_{n1} \end{bmatrix} \quad (26)$$

Here and henceforth an underline will denote the Voigt vector form of the relevant tensor. Note that from the Virtual Power Principle, it is

$$\mathbf{S} \cdot \delta\dot{\mathbf{E}} = \underline{\mathbf{S}} \cdot \mathbf{B}_0^T \delta\underline{\dot{\mathbf{a}}} = \mathbf{B}_0 \underline{\mathbf{S}} \cdot \delta\underline{\dot{\mathbf{a}}} \quad (27)$$

where $\underline{\mathbf{S}}$ is the Second Piola Kirchhoff stress tensor in Voigt notation. Therefore $\mathbf{B}_0\underline{\mathbf{S}}$ is the consistent discretization of the internal forces. Similarly for the identity

$$\tau \cdot \delta\mathbf{d} = \underline{\tau} \cdot \mathbf{B}_\Omega^T \delta\underline{\dot{\mathbf{a}}} = \mathbf{B}_\Omega \underline{\tau} \cdot \delta\underline{\dot{\mathbf{a}}} \quad (28)$$

it follows that the consistent discretisation of the internal forces in the spatial configuration is $\mathbf{B}_\Omega \underline{\tau}$ ($\underline{\tau}$ in Voigt notation).

Internal nodal forces and tangent stiffness

Two schemes are presented for determining the equivalent nodal forces and the stiffness matrices: a Total Lagrangian (TL) and an Updated Lagrangian (UL) formulation. In the former material objects are used, while in the latter spatial quantities are used. These

approaches are equivalent and substantially differ only on the numerical point of view. For determining the nodal forces let us start from the virtual power expression. Using (23)-(25) and indicating by δ virtual quantities one has

$$
\begin{array}{cc}
TL & UL
\end{array}
$$

$$
\begin{aligned}
\delta P^{\text{int}} &= \int_{V0} \mathbf{P} \cdot \delta \dot{\mathbf{F}}^T \, dV_0 = \int_{V0} P_{ij} \, \delta \dot{F}_{ij} \, dV_0 & \delta P^{\text{int}} &= \int_V \sigma \cdot \delta \mathbf{l} \, dV = \int_V \sigma_{ij} \, \delta l_{ij} \, dV \\
&= \int_{V0} P_{ij} \delta \dot{\mathbf{a}}_{i_k} \overline{B}_{kj} \, dV_0 = & &= \int_V \sigma_{ij} F_{ki}^{-1} \overline{B}_{lk} \delta \dot{\mathbf{a}}_{j_l} \, dV = \\
&= \int_{V_0} P_{1j} \delta \dot{\mathbf{a}}_{1_k} \overline{B}_{kj} + P_{2j} \delta \dot{\mathbf{a}}_{2_k} \overline{B}_{kj} \, dV_0 = & &= \int_V \sigma_{1i} F_{ki}^{-1} \overline{B}_{lk} \delta \dot{\mathbf{a}}_{1l} + \sigma_{2i} F_{ki}^{-1} \overline{B}_{lk} \delta \dot{\mathbf{a}}_{2l} \, dV = \\
&= \int_{V_0} \left(\overline{\mathbf{B}} \mathbf{P}_1 \cdot \delta \dot{\mathbf{a}}_1 + \overline{\mathbf{B}} \mathbf{P}_2 \cdot \delta \dot{\mathbf{a}}_2 \right) dV_0 = & &= \int_V \overline{\mathbf{B}} \mathbf{F}^{-1} \underline{\sigma}_1 \delta \dot{\underline{\mathbf{a}}}_1 + \overline{\mathbf{B}} \mathbf{F}^{-1} \underline{\sigma}_2 \delta \dot{\underline{\mathbf{a}}}_2 \, dV = \\
&= \underline{\mathbf{f}}_1^{\text{int}} \cdot \delta \dot{\underline{\mathbf{a}}}_1 + \underline{\mathbf{f}}_2^{\text{int}} \cdot \delta \dot{\underline{\mathbf{a}}}_2 & &= \underline{\mathbf{f}}_1^{\text{int}} \cdot \delta \dot{\underline{\mathbf{a}}}_1 + \underline{\mathbf{f}}_2^{\text{int}} \cdot \delta \dot{\underline{\mathbf{a}}}_2
\end{aligned}
\tag{29}
$$

having introduced the vectors $\mathbf{P}_1 = (P_{11}, P_{12}), \mathbf{P}_2 = (P_{21}, P_{22})$, and similarly for σ_1, σ_2. Substituting the definitions

$$
\mathbf{P} = \mathbf{FS} \rightarrow \begin{bmatrix} \mathbf{P}_1^T \\ \mathbf{P}_2^T \end{bmatrix} = \begin{bmatrix} \left(\mathbf{S}\overline{\mathbf{B}}^T \underline{\mathbf{a}}_1 \right)^T \\ \left(\mathbf{S}\overline{\mathbf{B}}^T \underline{\mathbf{a}}_2 \right)^T \end{bmatrix}
\qquad \tau = J\sigma
\tag{30}
$$

$$
dV_0 = |J_0| dV_\xi \qquad\qquad dV = J|\mathbf{J}_0| dV_\xi
$$

the following expressions for the internal nodal forces are recovered in the two cases

$$
\underline{\mathbf{f}}_i^{\text{int}} = \int_{V_\xi} \overline{\mathbf{B}} \mathbf{S} \overline{\mathbf{B}}^T |J_0| dV_\xi \, \underline{\mathbf{a}}_i = \overline{\mathbf{K}} \underline{\mathbf{a}}_i \qquad\qquad \underline{\mathbf{f}}_i^{\text{int}} = \int_{V_\xi} \overline{\mathbf{B}} \mathbf{F}^{-1} \underline{\tau}_i |J_0| dV_\xi
$$

$$
\underline{\mathbf{f}}^{\text{int}} = \begin{bmatrix} \overline{\mathbf{K}} & 0 \\ 0 & \overline{\mathbf{K}} \end{bmatrix} \underline{\mathbf{a}} = \mathbf{K}^{geo} \underline{\mathbf{a}}
\tag{31}
$$

or using Voigt notation

$$
\underline{\mathbf{S}} = \begin{bmatrix} S_{11} \\ S_{22} \\ S_{12} \end{bmatrix} \qquad\qquad \underline{\tau} = \begin{bmatrix} \tau_{11} \\ \tau_{22} \\ \tau_{12} \end{bmatrix}
$$

$$
\underline{\mathbf{f}}^{\text{int}} = \int_{V_\xi} \mathbf{B}_0 \underline{\mathbf{S}} |J_0| dV_\xi \qquad\qquad \underline{\mathbf{f}}^{\text{int}} = \int_{V_\xi} \mathbf{B}_\Omega \underline{\tau} |J_0| dV_\xi
\tag{32}
$$

In the following the tangent stiffness matrix is computed either for total and updated Lagrangian formulations. Being f_{ji}^{int} the nodal force at the j-th node in the i-th direction, the material derivative of (31) in UL approach can be computed as

$$
\dot{f}_{ji}^{\text{int}} = \int_{V_\xi} \overline{B}_{jA} \left(\dot{\overline{\mathbf{F}^{-1}}} \tau + \mathbf{F}^{-1} \dot{\tau} \right)_{Ai} |J_0| dV_\xi
\tag{33}
$$

18

Using the relations

$$\overline{\dot{\mathbf{F}^{-1}}} = -\mathbf{F}^{-1}\dot{\mathbf{F}}\mathbf{F}^{-1} = -\mathbf{F}^{-1}\mathbf{l} \tag{34}$$

$$L_v\tau = \dot{\tau} - \mathbf{l}\tau - \tau\mathbf{l}^T \rightarrow \dot{\tau} = L_v\tau + \mathbf{l}\tau + \tau\mathbf{l}^T \tag{35}$$

equation (33) yields

$$
\begin{aligned}
\dot{f}_{ji}^{int} &= \int_{V_\xi} \overline{B}_{jA}\left(-\mathbf{F}^{-1}\mathbf{l}\tau + \mathbf{F}^{-1}\mathbf{l}\tau + \mathbf{F}^{-1}\tau\mathbf{l}^T + \mathbf{F}^{-1}L_v\tau\right)_{Ai}|\mathbf{J}_0|dV_\xi \\
&= \int_{V_\xi}\left(\overline{\mathbf{B}}\mathbf{F}^{-1}\tau\mathbf{l}^T\right)_{ji}|\mathbf{J}_0|dV_\xi + \int_{V_\xi}\left(\overline{\mathbf{B}}\mathbf{F}^{-1}L_v\tau\right)_{ji}|\mathbf{J}_0|dV_\xi =: \dot{f}_{ji}^{geo} + \dot{f}_{ji}^{mat}
\end{aligned} \tag{36}
$$

so that the total nodal force increment is the sum of a geometric and a material part. Using interpolation (24), the geometric increment gives the geometric tangent stiffness as follows

$$
\dot{\mathbf{f}}_i^{geo} = \int_{V_\xi} \overline{\mathbf{B}}\mathbf{F}^{-1}\tau\,\mathbf{F}^{-T}\overline{\mathbf{B}}^T|\mathbf{J}_0|dV_\xi\,\underline{\dot{\mathbf{a}}}_i \rightarrow \underline{\dot{\mathbf{f}}}^{geo} = \mathbf{K}^{geo}\,\underline{\dot{\mathbf{a}}}
$$

$$
\mathbf{K}^{geo} := \int_{V_\xi}\left[\begin{array}{cc} \overline{\mathbf{B}}\mathbf{F}^{-1}\tau\,\mathbf{F}^{-T}\overline{\mathbf{B}}^T & 0 \\ 0 & \overline{\mathbf{B}}\mathbf{F}^{-1}\tau\,\mathbf{F}^{-T}\overline{\mathbf{B}}^T \end{array}\right]|\mathbf{J}_0|dV_\xi \tag{37}
$$

Using definition (26) for $\mathbf{B}_\Omega$, the material increment in (36) can be written in Voigt notation as

$$\underline{\dot{\mathbf{f}}}^{mat} = \int_{V_\xi} \mathbf{B}_\Omega \underline{L_v\tau}|\mathbf{J}_0|dV_\xi \tag{sub(38)}$$

The variation of the stress tensors appearing in (32) are linear functionals of the dual deformation measure, so that it can be substituted by the following relation

$$\underline{L_v\tau} = [\mathbf{c}]\cdot\underline{\mathbf{d}} \tag{39}$$

The exact expression of the material tensor will be obtained in the next paragraph. Substituting the previous relation in sub(38) and using interpolation (25) one has after some algebra

$$\underline{\dot{\mathbf{f}}}^{int} = \int_{V_\xi} \mathbf{B}_\Omega[\mathbf{c}]\mathbf{B}_\Omega^T|\mathbf{J}_0|dV_\xi\,\underline{\dot{\mathbf{a}}} = \mathbf{K}^{mat}\,\underline{\dot{\mathbf{a}}}$$

$$\mathbf{K}^{mat} := \int_{V_\xi} \mathbf{B}_\Omega[\mathbf{c}]\mathbf{B}_\Omega^T|\mathbf{J}_0|dV_\xi \tag{40}$$

The total tangent stiffness matrix is the sum of the material and the geometric tangent stiffness, so that

$$\mathbf{K} = \mathbf{K}^{mat} + \mathbf{K}^{geo} \tag{41}$$

For the total Lagrangian formulation, the tangent stiffness can be computed starting from the material derivative of the nodal force in (31)

$$\underline{\dot{\mathbf{f}}}_i^{\text{int}} = \int_{V_\xi} \overline{\mathbf{B}} \mathbf{S} \overline{\mathbf{B}}^T |\mathbf{J}_0| dV_\xi \, \underline{\dot{\mathbf{a}}}_i + \int_{V_\xi} \overline{\mathbf{B}} \dot{\mathbf{S}} \overline{\mathbf{B}}^T |\mathbf{J}_0| dV_\xi \, \underline{\mathbf{a}}_i =: \underline{\dot{\mathbf{f}}}_i^{\text{geo}} + \underline{\dot{\mathbf{f}}}_i^{\text{mat}} \tag{42}$$

using the definition of $\mathbf{K}^{\text{geo}}$ in (31), the geometric increment of the nodal forces gives

$$\underline{\dot{\mathbf{f}}}^{\text{geo}} = \mathbf{K}^{\text{geo}} \underline{\dot{\mathbf{a}}} \tag{43}$$

while, using definition (26) of $\mathbf{B}_0$, the material rate can be expressed in Voigt notation as

$$\underline{\dot{\mathbf{f}}}^{\text{mat}} = \int_{V_\xi} \mathbf{B}_0 \underline{\dot{\mathbf{S}}} |\mathbf{J}_0| dV_\xi \tag{44}$$

in virtue of the following relations

$$\dot{\mathbf{E}} = \mathbf{F}^T \mathbf{dF} \tag{45}$$

$$\dot{\mathbf{S}} = \mathbf{F}^{-1} L_v \tau \, \mathbf{F}^{-T} \tag{46}$$

Analogously to (39) in the reference configuration in Voigt notation it is

$$\underline{\dot{\mathbf{S}}} = [\mathbf{C_0}] \cdot \underline{\dot{\mathbf{E}}} \tag{47}$$

The elastoplastic moduli $\mathbf{C_0}$ is the Pull-Back of the spatial fourth order tensor $\mathbf{c}$. Substituting (47) in (44) and using the interpolation (25) for $\underline{\dot{\mathbf{E}}}$ one has

$$\begin{aligned}
\underline{\dot{\mathbf{f}}}^{\text{mat}} &= \int_{V_\xi} \mathbf{B}_0 [\mathbf{C_0}] \mathbf{B}_0^T |\mathbf{J}_0| dV_\xi \, \underline{\dot{\mathbf{a}}} = \mathbf{K}^{\text{mat}} \underline{\dot{\mathbf{a}}} \\
\mathbf{K}^{\text{mat}} &:= \int_{V_\xi} \mathbf{B}_0 [\mathbf{C_0}] \mathbf{B}_0^T |\mathbf{J}_0| dV_\xi
\end{aligned} \tag{48}$$

The total tangent stiffness is equal to the sum of its geometric and material parts defined in (43) and (48) respectively.

It can be proved that the expressions of the material and geometric tangent stiffness matrices for TL and UL formulations coincide. For details see [3, 4].

The difference in the tangent stiffness matrices for the two formulations are that in $\mathbf{K}^{\text{mat}}$ appears either $\mathbf{B}_0$ or $\mathbf{B}_\Omega$, and that in $\mathbf{K}^{\text{geo}}$ in the UL formulation appears the matrix product $\mathbf{F}^{-1} \tau \, \mathbf{F}^{-T}$, that is equal to the second Piola Kirchhoff tensor $\mathbf{S}$. Therefore, apart from the implementation at the local constitutive level, the only relevant difference is in the calculation of the interpolation matrices B_0 and B_Ω. From Equation (26) it is seen that $\mathbf{B}_\Omega$ has a simpler structure than $\mathbf{B}_0$. In the numerical applications the UL formulation has been used.

MATERIAL TANGENT STIFFNESS OPERATOR

The material stiffness matrix $\mathbf{K}^{\text{mat}}$ (in the UL formulation) depends on the tangent spatial anelasti constitutive moduli $[\mathbf{c}]$ that relates the Lie derivative of the Kirchhoff stress tensor and the total velocity of deformation tensor

$$L_v \tau = [\mathbf{c}] \cdot \underline{\mathbf{d}} \tag{49}$$

The matrix $[\mathbf{c}]$ can be computed in the Gauss points using the analytical form of the tangent stiffness tensor, that can be found starting from the constitutive relations defined in the intermediate configuration in Eqs (17) and the relation (see [1])

$$\mathbf{d} = \mathbf{d}_e + \mathbf{d}_a = \mathsf{c}_e^{-1} \cdot L_v \tau + \dot{\beta} \nabla_\tau \tau_{max} \tag{50}$$

The process is anelastic if either $\tau_{max} = 0$ and $\dot{\tau}_{max} = 0$. Recalling the definition of the limit function $\hat{f}$ it is

$$\dot{\hat{f}}(\mathbf{S}_e) = 0 \rightarrow \nabla_{\mathbf{S}_e}(\hat{f}) : \dot{\mathbf{S}}_e = \nabla_{\mathbf{S}_e}(\hat{f}) : \mathsf{C} : \hat{\dot{\mathbf{d}}}_e = \nabla_{\mathbf{S}_e}(\hat{f}) : \mathsf{C} : (\mathbf{d} - \mathbf{d}_a) =$$
$$= \nabla_{\mathbf{S}_e}(\hat{f}) : \mathsf{C} : \mathbf{d} - \dot{\beta} \nabla_{\mathbf{S}_e}(\hat{f}) : \mathsf{C} : \nabla_{\mathbf{S}_e}(\hat{f}) = 0 \tag{51}$$

Solving Eq (51) with respect to $\dot{\beta}$, one has

$$\dot{\beta} = \frac{\nabla_{\mathbf{S}_e}(\hat{f}) : \mathsf{C}}{\nabla_{\mathbf{S}_e}(\hat{f}) : \mathsf{C} : \nabla_{\mathbf{S}_e}(\hat{f})} \cdot \mathbf{d} \tag{52}$$

The previous relation allows to relate the material derivative of $\mathbf{S}_e$ to the total velocity of deformation

$$\dot{\mathbf{S}}_e = \mathsf{C} : \hat{\dot{\mathbf{d}}}_e = \mathsf{C} : \left(\hat{\dot{\mathbf{d}}} - \hat{\dot{\mathbf{d}}}_a \right) = \mathsf{C} : \hat{\dot{\mathbf{d}}} - (\mathsf{C} : \nabla_{\mathbf{S}_e}(\hat{f})) \frac{\nabla_{\mathbf{S}_e}(\hat{f}) : \mathsf{C}}{\nabla_{\mathbf{S}_e}(\hat{f}) : \mathsf{C} : \nabla_{\mathbf{S}_e}(\hat{f})} \cdot \mathbf{d} =$$
$$= \left(\mathsf{C} - \frac{(\mathsf{C} : \nabla_{\mathbf{S}_e}(\hat{f})) \otimes (\nabla_{\mathbf{S}_e}(\hat{f}) : \mathsf{C})}{\nabla_{\mathbf{S}_e}(\hat{f}) : \mathsf{C} : \nabla_{\mathbf{S}_e}(\hat{f})} \right) \cdot \hat{\dot{\mathbf{d}}} \tag{53}$$

From this result and Equation (12) the anelastic Lie derivative of $\mathbf{S}_e$ takes the form

$$L_v^p \mathbf{S}_e = \dot{\mathbf{S}}_e - \hat{\mathbf{l}}_a \tau - \tau \hat{\mathbf{l}}_a^T = \dot{\mathbf{S}}_e - \dot{\beta} (\nabla_{\mathbf{S}_e}(\hat{f}) \mathbf{S}_e + \mathbf{S}_e \nabla_{\mathbf{S}_e}(\hat{f})) =$$
$$= \left(\mathsf{C} - \frac{(\mathsf{C} : \nabla_{\mathbf{S}_e}(\hat{f})) \otimes (\nabla_{\mathbf{S}_e}(\hat{f}) : \mathsf{C})}{\nabla_{\mathbf{S}_e}(\hat{f}) : \mathsf{C} : \nabla_{\mathbf{S}_e}(\hat{f})} - \frac{(\nabla_{\mathbf{S}_e}(\hat{f}) \mathbf{S}_e + \mathbf{S}_e \nabla_{\mathbf{S}_e}(\hat{f})) \otimes (\nabla_{\mathbf{S}_e}(\hat{f}) : \mathsf{C})}{\nabla_{\mathbf{S}_e}(\hat{f}) : \mathsf{C} : \nabla_{\mathbf{S}_e}(\hat{f})} \right) \cdot \hat{\dot{\mathbf{d}}} = \tag{54}$$
$$=: \tilde{\mathsf{C}} \cdot \hat{\dot{\mathbf{d}}}$$

The expression of the spatial tangent stiffness, that relates the Lie derivative of the Kirchhoff stress tensor and the gradient of deformation tensor, is obtained pushing forward $L_v^p \mathbf{S}_e$, so it is found

$$\mathsf{c} = \phi_{e*}(\tilde{\mathsf{C}}) =$$
$$= \mathsf{c}_e - \frac{(\mathsf{c}_e : \nabla_\tau(f)) \otimes (\nabla_\tau(f) : \mathsf{c}_e)}{\nabla_\tau(f) : \mathsf{c}_e : \nabla_\tau(f)} - \frac{(\nabla_\tau(f) \tau + \tau \nabla_\tau(f)) \otimes (\nabla_\tau(f) : \mathsf{c}_e)}{\nabla_\tau(f) : \mathsf{c}_e : \nabla_\tau(f)} \tag{55}$$

In (55) the last term vanishes thanks to (16).
The previous equation represents the expression of the spatial material tangent stiffness.

In Eqn. (55) appear the stress and the elastic deformation tensor $\mathbf{C}_e$ (implicit in the elastic tensor) at the end of the step. These are numerically evaluated enforcing compatibility at the end of the step, integrating the constitutive model considering a sequence of finite steps t_1, t_2, …, t_n,… and approximating the time derivatives with finite increments. The material derivative of the Cauchy deformation tensor is written as:

$$\dot{\mathbf{C}}_{n,n+1}\,\Delta t = \mathbf{C}_{n+1} - \mathbf{C}_n$$
$$\mathbf{C}_{n+\alpha} = \mathbf{C}_n + \alpha\,\dot{\mathbf{C}}_{n,n+1}\,\Delta t \qquad \alpha \in [0,1] \qquad (56)$$

The computational procedure is described in detail in [6]. The problem has been solved by a consistent Newton's linearisation whose algorithmic consistent tangent operator is

$$\mathbf{H} = \begin{bmatrix} \nabla_{\underline{\tau}}\underline{\mathbf{e}} & \nabla_{\underline{\tau}}\tau_{n\max} & \nabla_{I_{3n+\alpha}^e}\underline{\mathbf{e}} \\ \nabla_{\underline{\tau}}\tau_{n\max} & 0 & 0 \\ \nabla_{\underline{\tau}}r_I & \nabla_{\beta}\,r_I & 1 \end{bmatrix} \qquad (57)$$

with

$$\mathbf{e}_{n+1} = \frac{1}{2}\left[\mathbf{I} - \left(\mathbf{f}_{n+1}\,\mathbf{f}_{n+1}^T\right)^{-1}\right] \qquad \mathbf{f}_{n+1} = \mathbf{F}_{n+1}\mathbf{F}_n^{-1}$$
$$r_I = -\left[I_{3n+\alpha}^e - \det\!\left(\mathbf{C}_{a\,n+\alpha}^{-1}\,\mathbf{C}_{n+\alpha}\right)\right] \qquad I_{3n+\alpha}^e = \det\!\left(\mathbf{C}_{n+\alpha}^e\right) \qquad (58)$$

The first row of (57) is the gradient of the compatibility conditions, the second is the gradient of the admissibility condition, while the last row has been added for iteratively evaluating the third invariant of the elastic Cauchy-Green tensor, that appears in the expression of the elastic tensor. As a matter of fact, as can be seen from (58), only the anelastic part of the Cauchy-Green tensor is explicitly known, since it is related to the anelastic velocity of deformation (details can be found in [6]).

In the calculation it has been used $\alpha=1$, so that the intermediate reference configuration coincides with the congruent one at the end of the step. However it has been proved by Simo [7] that the algorithm is objective for any choice of $\alpha \in [0, 1]$.

APPLICATIONS

The proposed model has been applied to the circular arch prototype represented in Figure 2. The arch, that is clamped at the bases, is loaded by an horizontal concentrated load, as shown in the figure. Its external and internal radii are 50 cm and 40 cm, respectively. The constitutive constants for the material λ, μ (see the hyperelastic potential reported in [1]) has been set in such a way that in the linear range they correspond to a Young modulus E = 10000 MPa and a Poisson ratio ν = 0.1, typical of soft stone masonry. Particularly it has been set $\lambda = 1136$ MPa and $\mu = 4545$ MPa. A unitary depth has been considered.
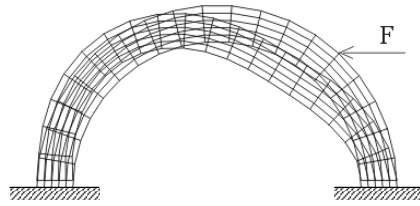
Figure 2. Circular Arch: geometry and load condition

This case is a significant test, since in masonry arches the formation of fractures results in hinges that cause large movements of the blocks. In Figure 3 the horizontal displacement of the point where the load is applied is plotted vs. the load itself. The result obtained with the present model (solid line) has been compared with the result of a large deformation totally elastic model (light line) and with the displacements obtained analyzing the arch with the concrete model implemented in ADINA using as limit stress in tension a nearly zero value (10^{-7} MPa) and an extremely large value for the limit compression stress in order to match the constitutive hypothesis of the present model. The ADINA model assumes small deformation and large rotations (dotted line). It is apparent that the present model accounts better for the non linearity of the response. In other words the non linear response of the model is only partially due to material non linearity, and even large rotations are not sufficient to correctly represent the deformation of the arch. This is due to the fact that, even if elastic strains in masonry materials are generally small, overall deformations due to fracture opening, can be locally quite large, as it occurs in the hinges that form in the arch. This result, in the opinion of the authors, motivates the efforts spent in extending the NTM model to finite deformations as well as the development of a fully geometrical non linear framework.
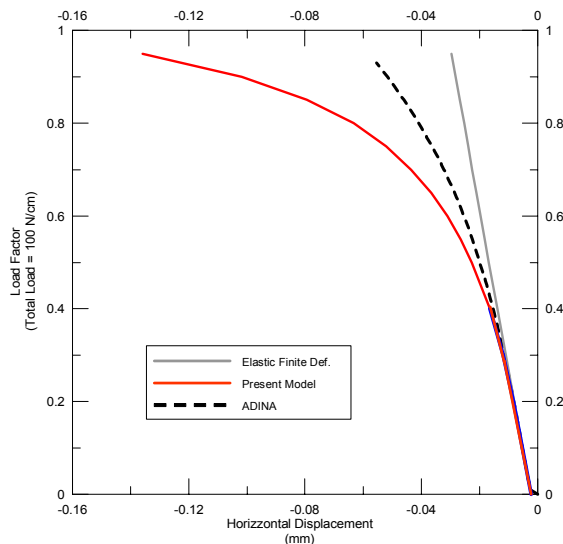

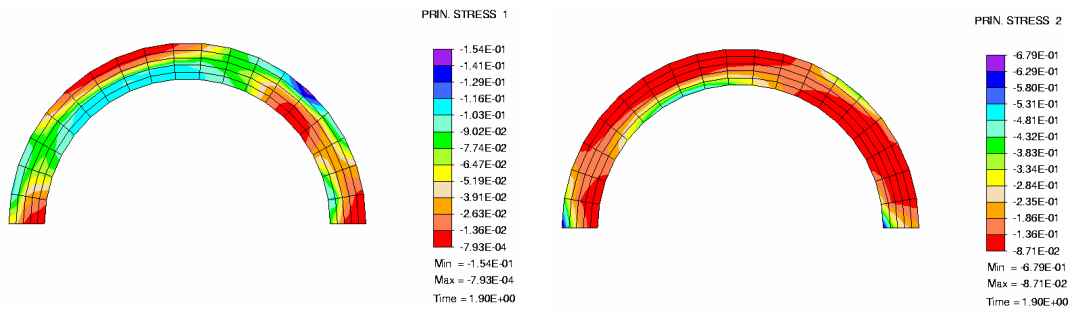**Figure 3.** Circular arch: horizontal displacement of the loaded point vs. load

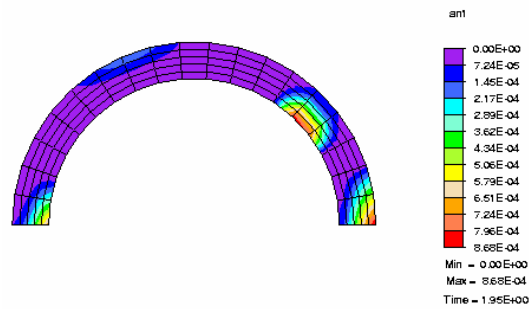**Figure 4.** Circular arch: principal stresses

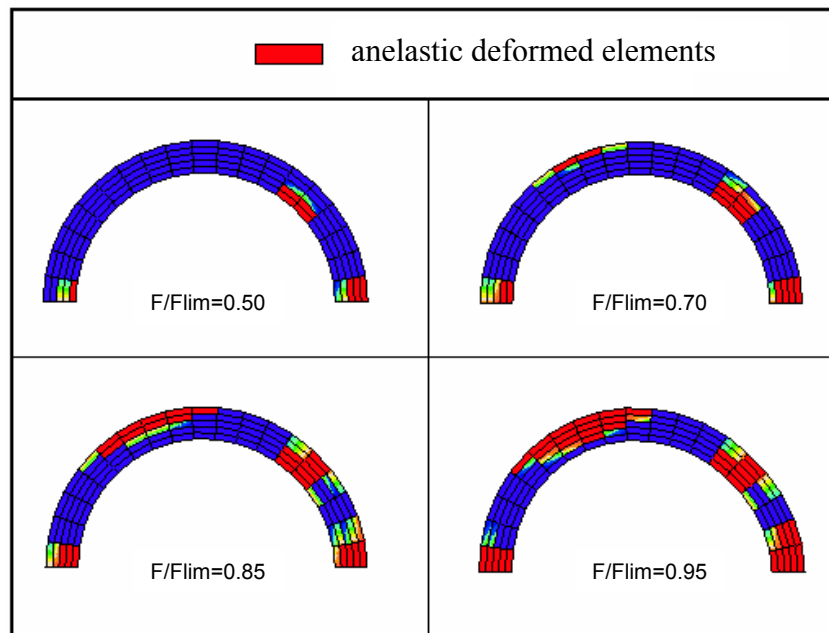**Figure 5.** Circular arch: maximum anelastic deformations

Figure 6. Circular arch: evolution of anelastic deformations

The distribution of principal stresses relative to the final state presents in Figure 4 shows the typical path of the pressure lines and zero stress areas where fractures develop, that is where the anelastic deformations are located. This is shown in Figure 5 where

24

anelastic deformations are plotted in terms of the maximum eigenvalue of the tensor

$$\mathbf{E}_a = \frac{1}{2}(\mathbf{C}_a - \mathbf{I}).$$

The inelastic deformations tend to concentrate in four zones, where inelastic hinges will develop leading to the collapse mechanism of the structure. The evolution of such anelastic hinges is described in Figure 6, for different values of the load.

A further application concerns the study of four panels with different aspect ratio (b/h = 0.67, 1, 1.33, 2) loaded by an uniform vertical pressure of 0.25 MPa and an horizontal pressure incremented until the limit of convergence, both applied at the top of the panels where it has been supposed that there is an elastic reinforcement. Anelastic deformations develop in zones of zero stress localized, for all the samples, in the centre and in the lower left corner (see Figure 7). As in the previous case, the anelastic and the total deformations are of the same order of magnitude and they are localised in the same areas of the samples. The top horizontal load vs. the top horizontal displacement is plotted for all the panels in Figure 8. It is apparent that the more slender panel has a more pronounced nonlinear behaviour.
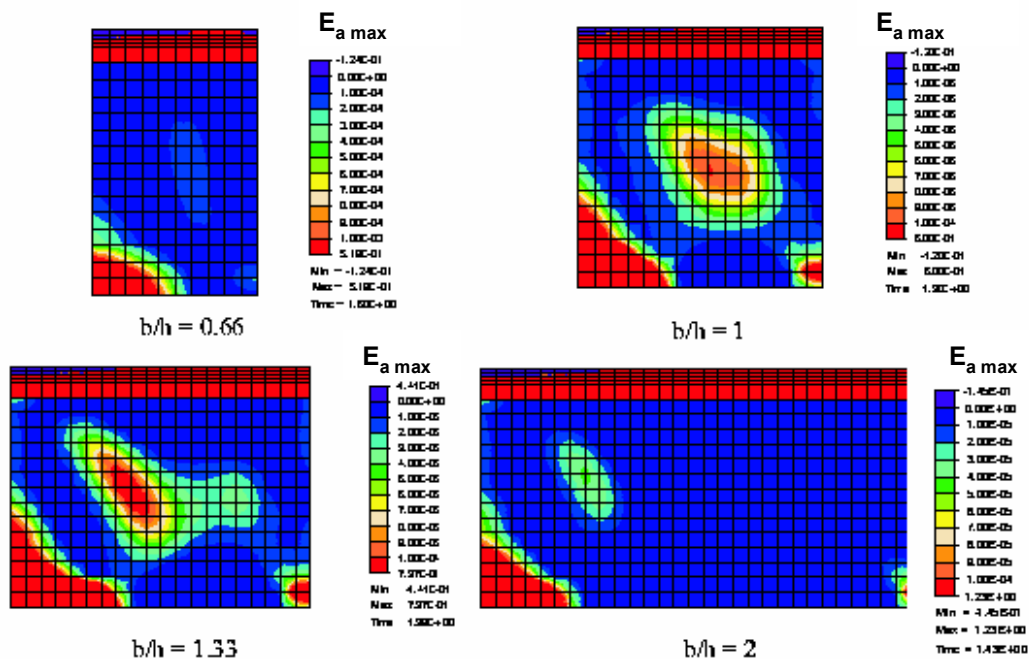

Figure 7. Shear panels: Maximum anelastic deformations

For the slender panel has been carried out also a displacement driven test performed imposing a vertical displacement at the top of the panel elastically equivalent to the pressure imposed in the previous analysis, subsequently the rotation of the top line has been prevented and an horizontal displacement has been imposed until the limit convergence is reached, when anelastic deformations have developed all throughout the sample. The evolution of the anelastic deformations for 3 values of the imposed displacement are reported in Figure 9. They present their maximum value at the centre

of the specimen, and, differently from the previous case, a non-straight fracture band appears.
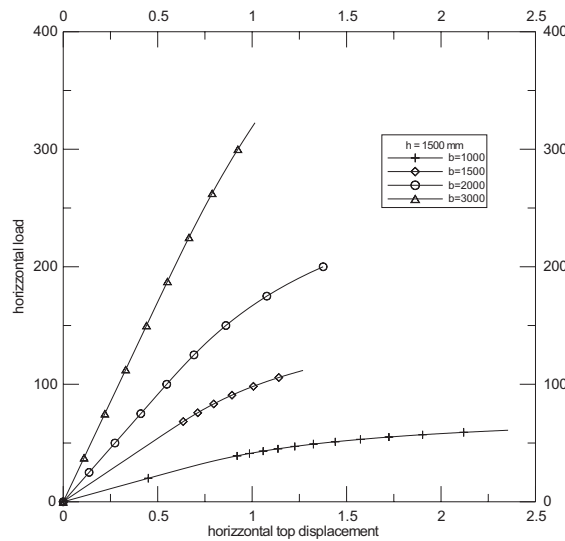

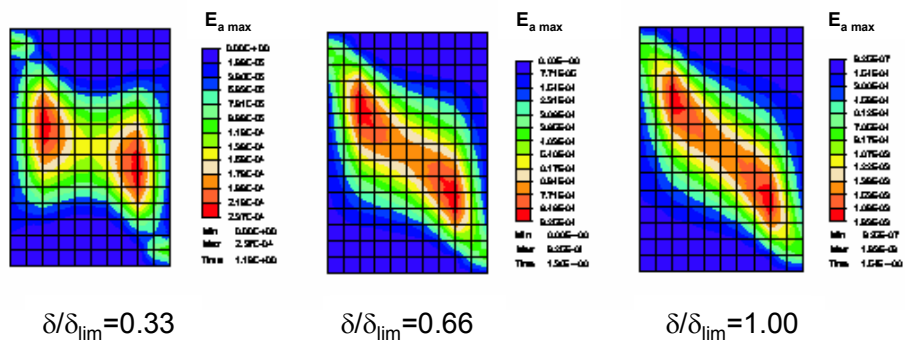**Figure 8.** Shear panels: Horizontal load vs. horizontal displacement

δ/δ_{lim}=0.33 δ/δ_{lim}=0.66 δ/δ_{lim}=1.00

Figure 9. Shear panels: Evolution of maximum anelastic deformations.

CONCLUSIONS

In this paper the FE implementation of a constitutive model for unilateral (no tension) materials in finite deformation is reported. The numerical model has been implemented in a FE code following either a Total Lagrangian (TL) or an Updated Lagrangian (UL) formulation. For both the formulations the expressions of the internal nodal forces, of the stiffness matrix and of the interpolating relations are reported. It can be proved that TL and UL approaches coincide.

Some applications have shown that the model indeed extends to large deformations the results obtained using the NTM model in small deformations. The numerical formulation appears to be robust, although it employs the exact expression of the

tangent stiffness operator in the material stiffness matrix, and not the consistent algorithmic expression, that is more difficult to evaluate.

REFERENCES

1. Cuomo M, Fagone M. A Numerical Model for Unilateral Materials, Part I: finite deformation modelling and numerical integration scheme. Submitted to Structural Mechanics, 2004
2. M. Fagone. Un modello computazionale per materiali inelastici in deformazione finita, PhD Thesis. D.I.C.A. University of Catania, december 2003.
3. Cuomo M, Fagone M. A Finite Element Formulation for Unilateral Materials in Finite Deformations. AIMETA, XV National Conference, Taormina, 2001.
4. Belytschko T, Liu WK. Moran B. Nonlinear Finite Elements for Continua and Structures. John Wiley & Sons Ltd, Chichester, England, 2000.
5. Marsden JE Hughes TJR. Mathematical Foundations of Elasticity, Dover, 1983.
6. Cuomo M, Fagone M. Constitutive Model for No Tension Materials in Finite Deformations. XIV National Conference of Computational Machanics, Brescia, 2000.
7. Simo JC, Hughes TJR. Computational Inelasticity. Springer 1998.

Massimo Cuomo, Full Professor   University of Catania, Department of Civil and Environmental Engineering, v.le A. Doria, 6, 95125 – Catania, Italy
Email: mcuomo@dica.unict.it

Mario Fagone, PhD   University of Catania, Department of Civil and Environmental Engineering, v.le A. Doria, 6, 95125 – Catania, Italy

Email: mfagone@dica.unict.it